TABLE III
RECOGNITION SCORES FOR THE DETECTION OF RIGHT AND LEFT IMAGINED MOVEMENTS IN 13 SUBJECTS. PERCENTAGES OBTAINED WITH THE DIFFERENT COMBINATIONS OF CLASSIFIERS (MAHALANOBIS-BASED WITH FULL, MAF, OR DIAGONAL, MAD, MATRIX, AND SSP) AND TWO OR FOUR ELECTRODES ARE LISTED

Subj.	SSP	SSP4	MAD2	MAD4	MAF2	MAF4
A.C.	38.8	46.1	37.8	34.5	93.5	98.8
C.T.	47.2	50.3	46.7	59.4	99.0	99.7
E.A.	49.2	50.5	52.0	50.2	99.4	99.7
E.V.	38.6	37.8	38.4	37.4	95.0	99.2
F.B.	61.6	63.7	72.9	79.1	98.9	99.0
F.C.	47.0	49.6	48.0	54.1	95.4	99.3
F.S.	51.3	59.3	56.0	69.3	98.7	99.1
G.C.	60.3	65.5	56.6	56.6	99.6	99.6
L.B.	48.6	57.8	44.5	58.2	96.8	98.7
L.P.	43.7	47.9	40.8	42.0	99.5	99.5
N.L.	45.6	52.9	50.2	57.5	94.6	99.4
R.L.	47.4	55.4	48.4	55.0	95.8	99.8
V.G.	45.2	53.6	57.02	68.8	98.9	99.1
	48.0	**53.1**	**49.9**	**55.6**	**97.3**	**99.3**

patterns is the decrease/increase of the power spectrum with respect to a baseline period [1]–[3] Additionally, our findings suggest that mental activity can be reliably detected by preprocessing the EEG signal with a SL estimator, even when using only nine electrodes. Though the SL estimator used is not absolutely accurate due to the reduced number of electrodes, the linear combination of channels that implements SL estimation is likely to apply a favorable transformation in the features' space. This transformation would simplify the distribution of patterns representing the EEG power distribution corresponding to different mental tasks. These findings are in line with those already obtained in a previous study [4].

In this study, we demonstrated that for the purpose of controlling by EEG the movement of a cursor on a computer screen, an interelectrode distance of 6 cm returned SL estimations more efficient than those obtained with an interelectrode distance of 3 cm. The difference in performance between the SL9 and SL methods (presented in Table II) presumably indicates that the former was better matched to the topographical extent of the EEG control signal. This study suggests that reduction of the number of scalp electrodes is possible for BCI devices. We observed that in a rather large group of normal subjects (13), EEG activity related to the imagination of movements detected by two electrodes placed over C3 and C4 scalp positions can be discriminated by a simple quadratic classifier. The characteristic property of the best performing classifier tested in this study is its ability to take into account the covariance of features' vectors. The evidence of higher recognition scores of this classifier may suggest that the spectral features used are actually correlated. This correlation should be taken into account in the classifier design to increase substantially the recognition scores.

The present result enlarges to a higher number of subject the observations made by Pfurtscheller *et al*. [2], also extending their results to normal subjects, whose cortical representation of the hand area, sampled from the two electrodes, is still intact and engaged in the network that allows the subject to control his muscles.

REFERENCES

[1] J. R. Wolpaw, N. Birbaumer, D. J. McFarland, G. Pfurtscheller, and T. M. Vaughan, "Brain-computer interfaces for communication and control," *Clin. Neurophysiol.*, vol. 113, pp. 767–791, 2002.

[2] G. Pfurtscheller, C. Guger, G. Muller, G. Krausz, and C. Neuper, "Brain oscillations control hand orthosis in a tetraplegic," *Neurosci. Lett.*, vol. 292, no. 3, pp. 211–214, 2000.

[3] B. Obermaier, C. Neuper, C. Guger, and G. Pfurtscheller, "Information transfer rate in a five-classes brain-computer interface," *IEEE Trans. Neural Syst. Rehab. Eng.*, vol. 9, pp. 283–288, Sept. 2001.

[4] D. J. McFarland, L. M. McCane, S. V. David, and J. R. Wolpaw, "Spatial filter selection for EEG-based communication," *Electroencephalogr. Clin. Neurophysiol.*, vol. 103, no. 3, pp. 386–394, 1997.

[5] G. Pfurtscheller and C. Neuper, "Motor imagery and direct brain-computer communication," *Proc. IEEE*, vol. 89, pp. 1123–1134, July 2001.

[6] P. D. Welch, "The use of fast Fourier transform for the estimation of power spectra: A method based on time averaging over short, modified periodograms," *IEEE Trans. Audio Electroacoustics*, vol. AU-15, pp. 70–73, June 1967.

[7] H. Zar, *Biostatistical Analysis*. New York: Prentice-Hall, 1984, ch. 10.

[8] F. Babiloni, F. Cincotti, L. Bianchi, G. Pirri, J. Millán, J. Mouriño, S. Salinari, and M. G. Marciani, "Recognition of imagined hand movements with low resolution surface laplacian and linear classifiers," *Med. Eng. Phys.*, vol. 328, pp. 323–328, 2001.

[9] F. Babiloni, F. Cincotti, L. Lazzarini, J. Millán, J. Mouriño, M. Varsta, J. Heikkonen, L. Bianchi, and M. G. Marciani, "Linear classification of low-resolution eeg patterns produced by imagined hand movements," *IEEE Trans. Rehab. Eng.*, vol. 8, pp. 186–188, June 2000.

[10] C. M. Bishop, *Neural Networks for Pattern Recognition*. Oxford, U.K.: Oxford Univ. Press, 1996, p. 35.

EEG Changes Accompanying Learned Regulation of 12-Hz EEG Activity

Arnaud Delorme and Scott Makeig

***Abstract*—We analyzed 15 sessions of 64-channel electroencephalographic (EEG) data recorded from a highly trained subject during sessions in which he attempted to regulate power at 12 Hz over his left- and right-central scalp to control the altitude of a cursor moving toward target boxes placed at the top-, middle-, or bottom-right of a computer screen. We used infomax independent component analysis (ICA) to decompose 64-channel EEG data from trials in which the subject successfully up- or down-regulated the measured EEG signals. Applying time-frequency analysis to the time courses of activity of several of the resulting 64 independent EEG components revealed that successful regulation of the measured activity was accompanied by extensive, asymmetrical changes in power and coherence, at both nearby and distant frequencies, in several parts of cortex. A more complete understanding of these phenomena could help to explain the nature and locus of learned regulation of EEG rhythms and might also suggest ways to further optimize the performance of brain-computer interfaces.**

***Index Terms*—Brain–computer interface (BCI), electroencephalogram (EEG), independent component analysis (ICA), μ rhythm.**

I. INTRODUCTION

When we alternately raise and then lower our arm at will, we have little awareness of the fact that these two actions involve complex coordination of activity in different sets of muscles. When a trained subject operating a brain–computer interface (BCI) raises or lowers, at will, a

Manuscript received July 15, 2002; revised January 26, 2003. This work was supported by the National Institutes of Health and by The Swartz Foundation.

The authors are with the Swartz Center for Computational Neuroscience, Institute for Neural Computation, University of California at San Diego, La Jolla, CA 92093-0961 USA (e-mail: arno@salk.edu; smakeig@ucsd.edu).

Digital Object Identifier 10.1109/TNSRE.2003.814428

particular amplitude measure of their electroencephalographic (EEG) signals (without producing muscle activity), are the changes produced in their EEG dynamics similarly complex? In particular, does up- and down-regulation of a specific EEG measure produce or involve other changes in their EEG dynamics? Answers to these questions might shed light on the fundamental nature and locus of learned EEG control and might also be used to guide the development of optimal BCI algorithms.

II. Methods

We analyzed 15 half-hour BCI sessions conducted in the Wolpaw group laboratory [1], [2], on a single highly-trained male subject (HK). In these experiments, changes in the amplitude of 12-Hz EEG power at left-central C3 electrode summed with the 12-Hz power at right central C4 electrode produced proportional changes in the screen height of a left-to-right moving cursor during experiments in which the subject attempted to make the cursor reach a goal box placed at the top, middle, or bottom right of a computer screen. Here, we report results for approximately 1000 successful top (up-regulate) and 1000 successful bottom (down-regulate) trials. Here, for simplicity, we omit results for the maintain-level trials. Further details of the experimental methodology are available elsewhere [3]. The sessions analyzed were numbers 196–210 for this subject, who at the time of these sessions had participated in similar experiments twice weekly for over two years. The frequency and scalp loci of the indicator rhythm used by the BCI algorithm had been hand tuned during previous sessions to optimize subject performance on the task, which during these sessions was consistent (up, 81% successful; down, 79%; chance level, 33%).

We used infomax independent component analysis (ICA) [4], [5] to decompose the 64-channel whole-scalp recordings into 64 maximally independent components. Many of these components accounted for eye or scalp muscle activity, or for single- or multichannel noise. We selected several of the larger components for detailed analysis using the EEGLAB Matlab toolbox [6]. One of these (the ninth largest by variance accounted for) clearly displayed characteristics of a right-hemisphere μ-rhythm generator, with its characteristic 11- and 22-Hz spectral peaks. The scalp map representing the projection of this component to the electrodes resembled closely the projection of a single dipole; BESA [7] source analysis showed that a single dipole in a spherical head model accounted for 97.8% of the scalp map variance. The resulting dipole was located near to the typical hand area of motor cortex, in line with previous results of ICA decomposition in button-press tasks [8] and with detailed investigations of μ-rhythm generators [9]. Other components we analyzed accounted for independent posterior alpha activities and for activity with 5- and 8-Hz peaks projecting to frontocentral cortex. The scalp maps of these components could also be fit by a single dipole with 4%–6% residual variance. To study the concomitant dynamics of each of these components during learned μ-rhythm regulation, we computed erp-image plots [10], and event-related spectral perturbation (ERSP) [11] and event-related coherence images [12].

III. Results

Fig. 1(b) shows that while power at the 12-Hz regulation frequency is distributed across the head, the spatial pattern of 12-Hz regulation is maximal near C3, with a second maximum near C4. During up-regulation, 12-Hz power is higher than during down-regulation at all channels except over right prefrontal scalp [Fig. 1(a)]. Fig. 1(c) demonstrates that relative to down-regulation, up-regulation is associated with increased power at C3 and at C4 across the EEG frequency range, with a difference maximum at 12 Hz and smaller peak differences near 2, 4, 22, and 38 Hz. Near 12 and 22 Hz, the regulation effect is stronger at C3 than C4; at other frequencies it is equal at both channels.

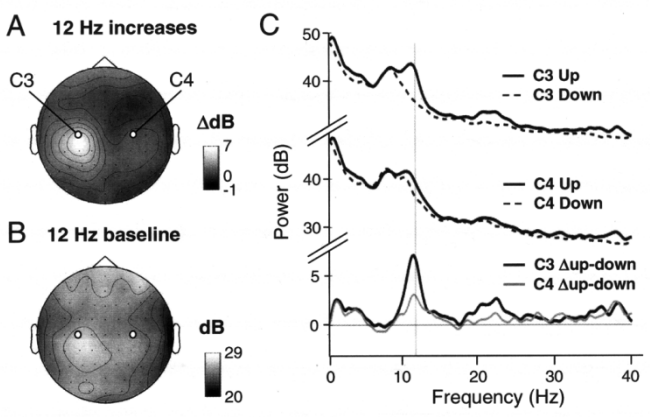

Fig. 1. Effects of learned regulation on EEG spectral power of a highly trained subject performing a BCI experiment in which summed changes in EEG power near 12 Hz at sites C3 and C4 were used to adjust the screen height of a moving cursor. In each trial, the target box appeared at time 0, and the cursor at 1.5 s. The subject's task was to make the cursor move into a box placed at the right top or bottom of the screen. (A) Power difference at 12 Hz during active regulation (up-regulate minus down-regulate, 800–2000 ms). (B) Distribution of 12-Hz power at baseline (0–500 ms). (C) Power spectra during regulation (800–2000 ms) at C3 and C4. Note that during up-regulation, EEG power is larger at nearly all frequencies than during down-regulation (lower traces).

To explore the spatial and frequency-domain extent of the effects of EEG egulation, we analyzed activity of several independent EEG components accounting for portions of 12-Hz power at C3 and C4. Fig. 2 shows the mean and trial-length sorted and smoothed single-trial time courses of power around 12 Hz in the right-μ component [mapped in Fig. 2(a)] in successful up- and down-regulate trials. During regulation (800–2000 ms), this component accounted for a mean of 27% of 12-Hz power at site C4 and 15% at C3.

In both conditions, the appearance of the target cue at 0 ms is followed by a dip in power peaking near 300 ms, with return to baseline in both trial types near 700 ms. Thereafter, the two power trajectories diverge until trial end (Fig. 2(c), curved lines). Following the end of the trial, amplitude decreases in both conditions. The two trajectories are not mirror images of each other, however. After an initial surge (at roughly 800–1100 ms), up-regulation is sustained for the trial duration (Fig. 2(c), top), whereas during down-regulation 12-Hz power returns nearly to baseline at about 2 s. Note that following down-regulate trials, 12-Hz power actually dips below its minimum down-regulated level.

Some concomitant effects of 12-Hz regulation on other EEG processes are shown in Fig. 3, which portrays, for three independent EEG components accounting for posterior alpha activities, trial-length sorted single-trial power trajectories at the frequency in the alpha band showing the largest event time-locked variability. Note that the up- and down-regulate trial trajectories for these components also differ from one another, with largest differences between conditions appearing *after* trial end.

Fig. 4 shows the concomitant effects of μ-rhythm regulation on other EEG frequencies in the right-μ component spectrum. For this component, 12-Hz regulation was accompanied or followed by modulations of power in narrow bands near 7, 11, 17, and 30 Hz. Power trajectories at these frequencies differed in several ways between up- and down-regulate conditions.

Fig. 5 shows that the changes in EEG dynamics accompanying μ-rhythm regulation included changes in partial phase coherence between maximally independent components accounting for independent posterior alpha rhythms [13]. These changes also differed in up- and down-regulate conditions. In particular, partial phase coherence at 12 Hz between these processes appeared to be stronger during

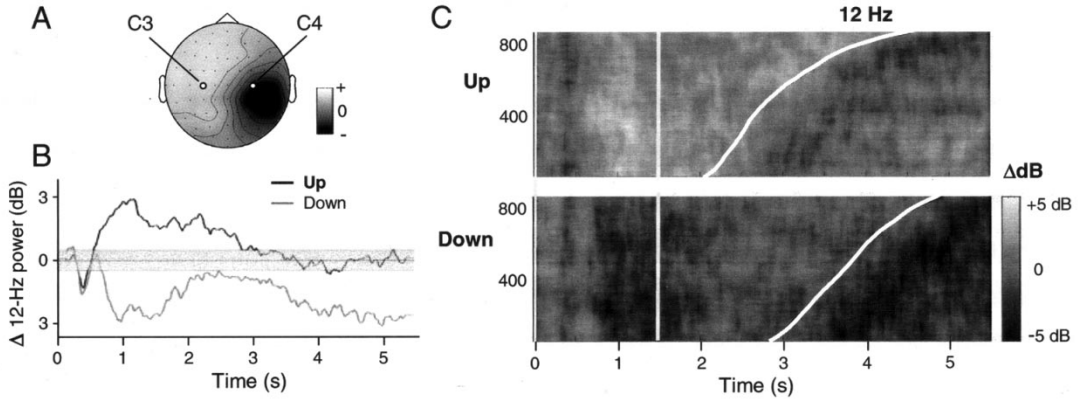

Fig. 2. Time course of relative spectral power at 12 Hz (by 3-cycle wavelets) in an independent EEG component accounting for μ-rhythm activity projecting most strongly to the right-central scalp. Same subject as in Fig. 1. (A) Scalp map showing the fixed pattern of projection of the component to the scalp electrodes. (B) Mean 12-Hz component power trajectories for the two trial conditions. The central grey band shows bootstrap power baseline and bootstrap significance limits ($p < 0.01$). (C) Time course of power at 12 Hz in 1000 single trials per condition sorted in order of trial duration and then smoothed vertically with a 100-trial moving average (curved lines show trial end; vertical axis: smoothed trial number).

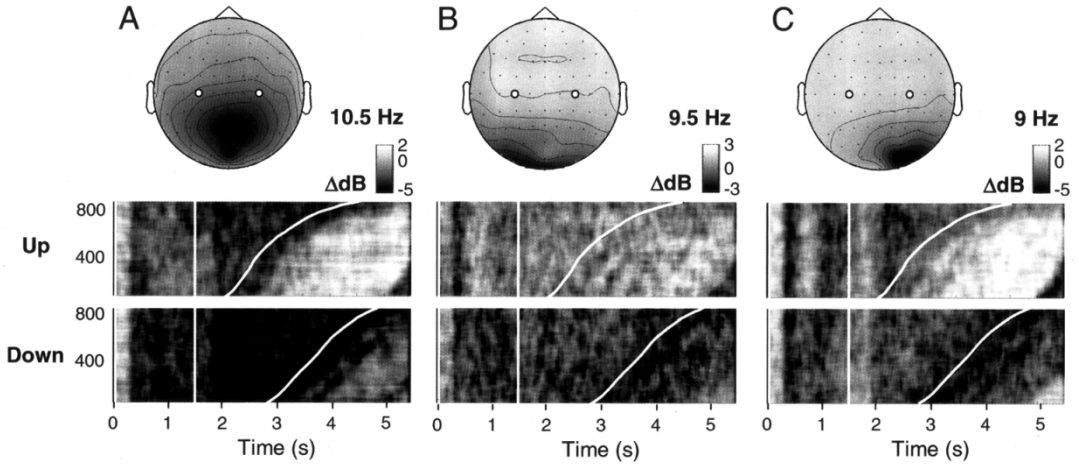

Fig. 3. Power trajectories for three independent EEG components in successful μ-rhythm up- and down-regulate trials. Same subject and trials as in Figs. 1 and 2. All three components have a peak in their activity spectrum near 10 Hz. (A) Power at 10.5 Hz in a central posterior alpha component, shows alpha block following target onset, stronger in down-regulate trials, particularly after cursor onset. After trial offset, power returns to baseline. (B) 9.5-Hz power in a left posterior alpha source, showing blocking after target onset (1.5 s) in down-regulate trials only. (C) 9-Hz power in a right posterior alpha source, showing phasic increases after target and cursor onsets and a power increase after offset of up-regulate trials only.

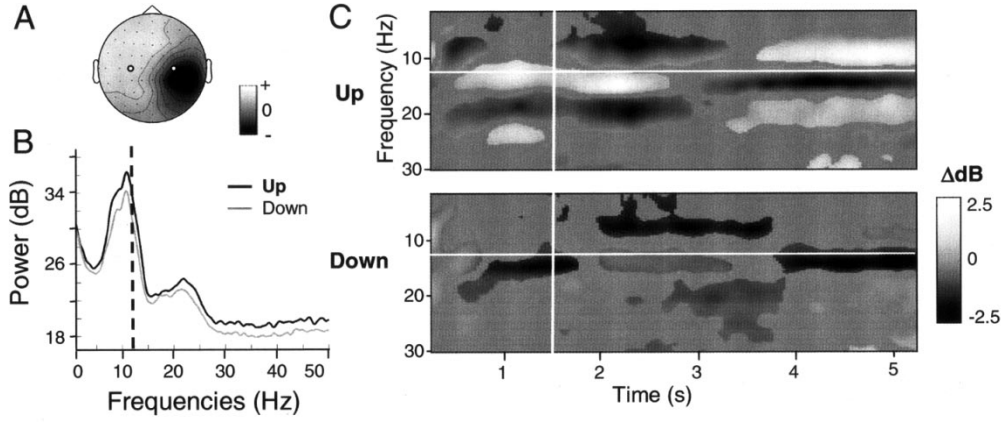

Fig. 4. Time/frequency decomposition (by FFT) of the right-μ independent component of Fig. 2 in successful up- and down-regulate trials. Bootstrap significance level: $p < 0.01$ (A) Scalp map showing the pattern of projection of the component to the scalp electrodes. (B) Mean power spectrum in up-regulate (black trace) and down-regulate (gray) trials. Dashed vertical line shows the 12-Hz frequency used to control cursor altitude. (C) Time-frequency decompositions for up- and down-regulate trials. In up-regulate trials, changes in 12-Hz power are accompanied by inverse changes in power near 7.5 and 20 Hz. In down-regulate trials, power decreases at 12–15 Hz are accompanied by a somewhat different set of amplitude modulations.

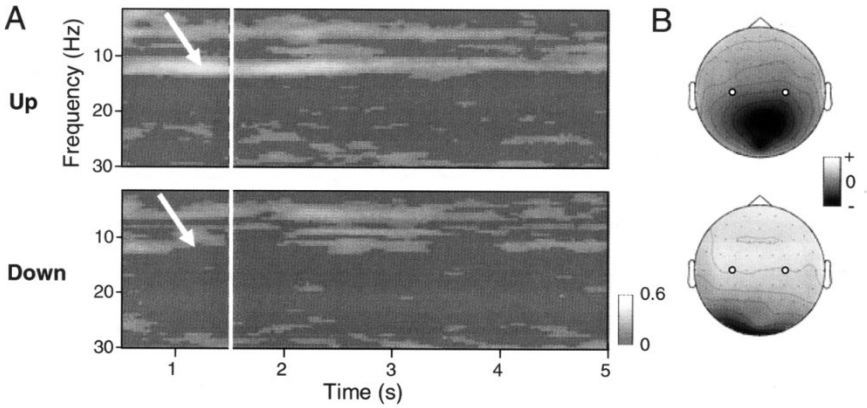

Fig. 5. Event-related phase coherence in successful μ-rhythm up- and down-regulate trials between two independent EEG components whose alpha-power time courses are shown in Fig. 3. (A) In up-regulate trials, 12-Hz phase coupling of the two components increases (top arrow) whereas in down-regulate trials it becomes insignificant (bottom arrow). Bootstrap significance level: $p < 0.01$. (B) Scalp maps showing the pattern of projection of the components to the scalp electrodes.

up-regulation than during down-regulation. Other phase coherence changes (not shown) were observed for other component pairs.

IV. Discussion

Clearly, while this highly trained subject regulated the amplitude of his 12-Hz EEG activity on the left- and right-central scalp, he simultaneously modulated his EEG dynamics at several cortical areas and frequencies. Therefore, learned modulation of one EEG amplitude measure may be effected through a process that concurrently modulates multiple EEG processes, producing event-related changes in power in multiple EEG components and frequencies. Many of the concomitant power changes in alpha rhythms resemble the broad so-called "event-related desynchronization" (ERD) blocking of alpha rhythms [14] seen in experiments involving focused attention [15]. Here, central posterior alpha [Fig. 3(a)] activity was blocked during both up- and down-regulation. Thus, the brain systems involved in regulating left- and right-μ activity in this subject are not located only in motor cortex. Instead, they may involve distributed arousal and attention networks, possibly linked to subcortical modulatory systems associated with nonglutaminergic transmission. In these sessions, up- and down-regulation of 12-Hz (μ) activity was also accompanied by changes in event-related coherence between maximally independent EEG component processes (Fig. 5).

Notably, many of these changes in EEG dynamics during learned regulation were asymmetric with respect to the direction of regulation. In particular, up-regulation, but not down-regulation, was followed by increases in three posterior alpha-generating processes (Fig. 3). Aspects of the time courses of power change in the μ-rhythm generating process, both at 12 Hz (Fig. 2) and at other frequencies (Fig. 4), were also asymmetric.

V. Conclusion

While the results presented here come from a single subject, they appear to have been consistent over fifteen separate sessions. The accumulating data archive of BCI laboratories using this and other paradigms presents a clear opportunity to study the independence and interdependence of dynamic changes in cortical synchronization that produces EEG signals [16]. In particular, it should be interesting to study the extent to which the spectral changes produced by trained BCI subjects become tuned to the exact algorithm used to effect operant control. ICA components representing several independent EEG processes accounted for activity at 12 Hz in the controlling channels in this subject.

Had this subject been trained to directly regulate the activity of an independent left- or right-hemisphere μ component, would the concomitant changes in other EEG processes differ from those shown here? Are there regularities in the location and dynamic portraits of those independent EEG components that co-vary with μ activity in BCI experiments? Answers to these and similar questions could reveal more about the function of EEG rhythms, and might suggest ways to incorporate more information about EEG dynamics into BCI algorithms (e.g., combining spectral measures of more than one independent component process), possibly improving their performance.

Acknowledgment

The authors wish to thank J. Wolpaw, D. McFarland, and T. Vaughan of the Wadsworth Center, Albany, NY, for sharing the data on which this report is based and for helpful discussions and suggestions.

References

[1] J. R. Wolpaw, D. J. McFarland, G. W. Neat, and C. A. Forneris, "An EEG-based brain-computer interface for cursor control," *Electroencephalogr. Clin. Neurophysiol.*, vol. 78, pp. 252–259, 1991.

[2] D. J. McFarland, L. M. McCane, S. V. David, and J. R. Wolpaw, "Spatial filter selection for EEG-based communication," *Electroencephalogr. Clin. Neurophysiol.*, vol. 103, pp. 386–394, 1997.

[3] D. J. McFarland and J. R. Wolpaw, "EEG-based communication and control: Speed-accuracy relashionships," *Appl. Psychophysiol. Biofeedback*, 2002, to be published.

[4] S. Makeig, A. J. Bell, T. P. Jung, and T. J. Sejnowski, "Independent component analysis of electroencephalographic data," in *Advances in Neural Information Processing Systems*, D. M. M. Touretzky and M. Hasselmo, Eds. Cambridge, MA: MIT Press, 1996, vol. 8, pp. 145–151.

[5] S. Makeig, S. Enghoff, T. P. Jung, and T. J. Sejnowski, "A natural basis for efficient brain-actuated control," *IEEE Trans. Rehab. Eng.*, vol. 8, pp. 208–211, June 2000.

[6] A. Delorme and S. Makeig. (2002) EEGLAB: A MATLAB toolbox for electrophysiological data analysis. Univ. California San Diego, Swartz Center for Computat. Neurosci., La Jolla, CA. [Online]. Available: http://sccn.ucsd.edu/eeglab/

[7] M. Scherg and P. Berg, "Use of prior knowledge in brain electromagnetic source analysis," *Brain Topogr.*, vol. 4, pp. 143–150, 1991.

[8] S. Makeig, M. Westerfield, T. P. Jung, S. Enghoff, J. Townsend, E. Courchesne, and T. J. Sejnowski, "Dynamic brain sources of visual evoked responses," *Science*, vol. 295, pp. 690–694, 2002.

[9] R. Hari, R. Salmelin, J. P. Makela, S. Salenius, and M. Helle, "Magnetoencephalographic cortical rhythms," *Int. J. Psychophysiol.*, vol. 26, pp. 51–62, 1997.

[10] T. P. Jung, S. Makeig, M. Westerfield, J. Townsend, E. Courchesne, and T. J. Sejnowski, "Analyzing and visualizing single-trial event-related potentials," *Adv. Neur. Inform. Process. Syst.*, vol. 11, pp. 118–124, 1999.